JOURNAL OF AIRCRAFT
Vol. 43, No. 4, July–August 2006

# Civil-Transport Wing Design Concept Exploiting New Technologies

Prasetyo Edi*
*University Putra Malaysia, Selangor DE. 43400, Malaysia*
and
J. P. Fielding†
*Cranfield University, Cranfield, England MK43 0AL, United Kingdom*

**Current trends in the design of transport aircraft have shown that in order to be economically viable and competitive it is necessary to investigate technologies that can give an improvement in performance and operational flexibility goal, but must be shown to be cost effective. The current competitive environment forces the airlines to buy advanced technology aircraft and requires manufacturers to provide more operational flexibility, without drastic performance penalties. This is a challenging task, which might be solved by the use of new technologies. It is believed that the application of a hybrid laminar-flow control (HLFC) and variable camber (VC) to a wing would assist in achieving such a task. This paper describes an investigation aimed to examine the suitability of an aerodynamic wing design, allowing for the use of a combined HLFC-VC concept for transonic transport aircraft. The paper describes the phenomenon of laminar flow and outlines the wing design process. It then discusses the benefits and penalties of the variable-camber wing concept. Description is then given of the aerodynamic design of a wing that incorporated both laminar-flow and variable-camber technologies. It concludes with a discussion of the results and recommendations for future work.**

## Nomenclature

| | | |
|---|---|---|
| $b$ | = | wing span |
| $C$ | = | chord/coefficient |
| $D$ | = | drag |
| $L$, 1 | = | Lift |
| $M$ | = | Mach number |
| $N$ | = | normal |
| $y$ | = | spanwise station |
| $\alpha$ | = | angle of attack |

*Subscript*

| | | |
|---|---|---|
| max | = | maximum |

*Superscript*

| | | |
|---|---|---|
| $\sim$ | = | freestream |

## I. Introduction

FOR commercial transport aircraft, one of the basic aerodynamic performance objectives is to achieve the highest value of $M(L/D)_{\max}$ at the cruise Mach number. Climb and descent performance, especially for short-range missions, is also important and can suggest the "cruise" design conditions be compromised. In the past 20 years, much airframe development has been aimed at reducing lift-dependent drag, leading to higher-aspect-ratio-wings and winglets coupled with overall optimization of wing design.[1]

To achieve further major advances, it is necessary to look at other aspects of design, in particular, the reduction of profile drag. Boundary-layer control, aimed at extending laminar flow over greater areas of the wing, has been pursued intermittently since the early days of aviation. Laminarization of other aircraft components such as tailplane, fin, and engine nacelle offers additional advantages.

Variable camber (VC) offers an opportunity to achieve considerable improvements in operational flexibility, buffet boundaries, and performance; it does this by increasing the lift/drag ratio in cruise and climb because the variable camber enables cruise and climb to be always at an optimum lift coefficient.[2]

This paper describes the continuation of previous work in these areas to assess their broad impact on wing design parameters to produce major increases in aerodynamic wing efficiency. It is based on the first author's Ph.D. research.[3]

## II. Advanced Technologies Studied

Two advanced technologies were investigated during this study, namely, laminar flow and variable-camber wing.

### A. Laminar Flow

There are three basic transition mechanisms on a swept wing. Viscous or Tollmien–Schlichting instability (T.S.I.), inflectional or crossflow instability (C.F.I.), and leading-edge attachment line transition. A laminar wing must optimize pressure gradients taking into account T.S.I. and C.F.I. The natural-laminar-flow (NLF) concept can only be applied to the following configurations: 1) low sweep and moderate Reynolds numbers and 2) high sweep and small Reynolds numbers. For the current high sweep and high Reynolds numbers encountered on large transport aircraft, it is necessary to maintain laminar flow by suction of the boundary layer over the entire wing surface [laminar-flow control (LFC)] or near the leading edge only [hybrid laminar-flow control (HLFC)].[4,5]

### B. Variable-Camber Wing (VCW)

From the beginning of aeronautics, aircraft have used wing camber and twist variation to alter lift characteristics and achieve lateral control. Most aircraft today mechanically change their low-camber, high cruise-speed wings into high-camber, low-speed wings for take-off, landing, and other operations. To date, the methods used are characterized by leading-edge and trailing-edge slat and flap systems that, in general, move in large increments with associated

Received 14 January 2005; revision received 31 May 2005; accepted for publication 22 June 2005. 

*Lecturer, Aerospace Engineering, Serdang; p_edi@eng.upm.edu.my.
†Professor of Aircraft Design, Head, Aerospace Engineering Group, Department of Power, Propulsion and Aerospace Engineering, School of Engineering; j.p.fielding@cranfield.ac.uk. Senior Member AIAA.

undesirable steps and gaps in both the high-camber and low-camber positions. The result is an airfoil that is never quite optimum for every flight condition and an excrescence drag that is appreciable under all conditions.[2]

A remarkable job of engineering has provided today's highly efficient civil transports with high ranges of speed and flight conditions. However, the spiraling cost of fuel requires renewed efforts to absolutely minimize the fuel consumed by these civil transports. In the area of camber-changing devices, structural and mechanical technology has advanced to where practical systems might be possible for changing the shape of an airfoil continuously and smoothly such that it is more nearly optimum for all flight conditions.[3,6]

## III. Wing Design

### A. General Requirements

Basic requirements that must be achieved for a successful wing design include the following:

1) The configuration must satisfy the performance goals in the design specifications while achieving good economic returns.

2) Flight characteristics, handling qualities, and aircraft operations must be satisfactory and safe over the entire flight envelope for all aircraft configurations (high speed, low speed, different flap settings, gear positions, power settings, and suitable ground handling).

3) Design of a structure must be possible within the defined external shape to meet the strength, torsion, fatigue, flutter, weight, life cycle, maintainability, accessibility, and engine requirements, together with suitable development and manufacturing costs.

4) Sufficient space must be provided for fuel for the design range, for retraction of the main landing gear, and for the aircraft systems (flaps, ailerons, spoilers, fuel, gear, etc.), where appropriate.

Meeting all of these requirements simultaneously is difficult and will most likely require compromise for a satisfactory configuration to be achieved. Parameters affecting wing design are presented in Fig. 1.

### B. Some Aerodynamic Design Considerations

*1. Wing Sweep Selection*

The application of laminar flow on swept wings is effectively limited at high Reynolds numbers by a high sweep angle, as crossflow instability and attachment line transition lead to fully turbulent boundary layers on the wing.[5] Theoretical and experimental investigations on finite swept wings show, because of three-dimensional displacement effects, an effective increase of wing sweep for rearward-swept wings and an effective decrease of wing sweep for forward-swept wings, compared to the geometrical sweep. For a laminar-flow wing, the reduction in sweep in the case of a forward-swept wing leads to a more stable laminar boundary layer concerning transition because of crossflow instability and attachment line transition. Thus, with this concept, a laminar forward-swept wing can be realized more easily than a comparable sweptback wing.[7]

For forward-swept wings the major technical disadvantages of a further outboard center of lift and the potential of divergence could possibly be overcome in the future using active load alleviation, variable camber, and/or composite tailoring designed to reduce bending and minimize center of pressure movement. There is little to choose between forwards/aft-swept wings in terms of nacelle integration. Stability and control characteristics of forward-swept wings are not well understood. The main problem of forward-swept wings is natural divergence and the tendency towards flutter.

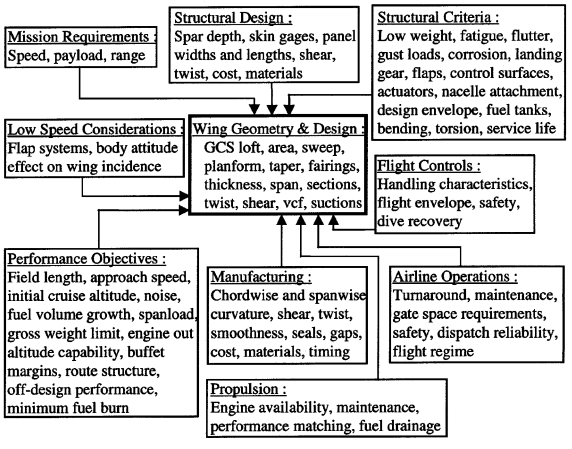


**Fig. 1 HLFC-VC wing design requirements and objectives.**

*2. HLFC-VCW Airfoil Design Criteria*

The introduction of laminar flow represents an additional design criterion that must be satisfied alongside existing considerations. The issues raised for NLF section design are also relevant to HLFC sections although leading-edge suction reduces the severity of the constraints imposed for NLF. Typical transonic HLFC aerofoil sections have been designed with pressure distributions having a small peak close to the leading edge, followed by a region of increasing pressure over the suction region, after which the "rooftop" has a mildly favorable pressure gradient. Such a pressure distribution has been found to maximize the extent of laminar flow.[4,8,9]

Development of an aerofoil is concerned mainly with the selection of the desired pressure distribution. Once this is done, the shape can be computed by a mathematical procedure. However, not all pressure distributions correspond to physically meaningful airfoil shapes; real flow constrains the pressure distribution to have a leading-edge stagnation point, low-pressure forward, and gradually rising pressure aft, ending somewhat above ambient at the trailing edge. Within these constraints, details must be tailored to meet the specific requirements of HLFC and of low drag rise caused by compressibility. The following points should be observed[10]:

A steep initial gradient (rapidly falling pressure) is helpful in preventing attachment line transition on a wing having substantial leading-edge sweepback. Wong and Maina[9] give the initial pressure gradients for an Airbus-type and a Pfenninger-type aerofoil.

The midchord pressure distribution affects susceptibility to the two other principal transition mechanisms. Falling pressure tends to suppress the growth of Tollmien–Schlichting disturbances, and rising pressure will generally promote their rapid amplification. Hence, a negative gradient (falling pressure) is often called "favorable," and a positive gradient (rising pressure) is termed "adverse." However, substantial gradients of either sign will combine with sweepback to produce boundary-layer crossflow, which tends to amplify disturbances and to promote transition. The favorable pressure gradient should not be so great as to avoid excessive loss of lift for a given shock strength compared to the turbulent design. The fundamental technical strategy of HLFC is to confine the unavoidable large negative gradients to the region ahead of the front spar and to use boundary-layer suction to suppress disturbance amplification as a result of crossflow there. Downstream of the front spar, gradients are kept in the weakly favorable to zero range.

The minimum pressure level on the upper surface must correspond to a slightly supersonic velocity on an efficient high-speed wing. To limit wave drag, the local Mach number has to be restricted to a value less than Mach 1.2. The shock strength at the return to subsonic flow must not be so great as to cause excessive wave drag or separation of the turbulent boundary layer.

Extended regions of favorable pressure gradient would correspond to extended regions of laminar flow. Therefore, it was required that the pressure gradients be favorable as far aft as the design transition points.

To ensure attached flow, the maximum slope of the upper- and lower-surface aft pressure gradient, $dC_p/d(x/c)_{max}$, is to be less than 3.0.

The pressure level on the lower surface is determined by the desired lift coefficient and airfoil thickness ratio.

The flow will normally remain subsonic and therefore shock free. A recovery region having an adverse pressure gradient and turbulent flow must occupy the aftmost portion.

To control the pressure gradients and the off-design behavior, HLFC is combined with variable-camber flaps. These design criteria are summarized in Fig. 2.

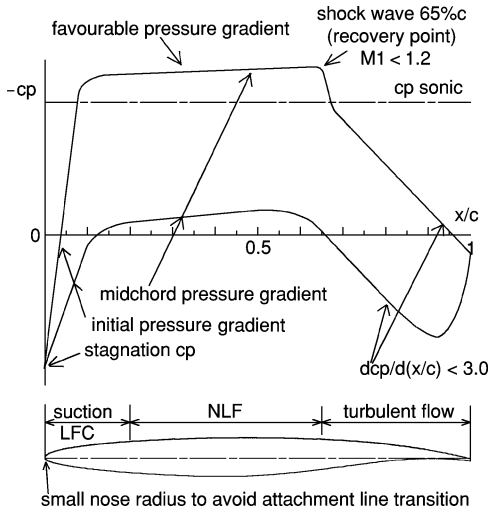


**Fig. 2 HLFC airfoil design criteria.**

The aerofoils just described, however, are often prone to increased shock growth, which results in earlier occurrence of drag rise conditions, relative to an aerofoil with an adverse rooftop pressure gradient. In fundamental wing design terms this implies increased sweep, reduced thickness/chord ratio, and/or reduced wing loading, all of which reduce the aerodynamic and/or structural efficiency of the wing for a specified design condition. An alternate approach might be to use an aerofoil with a mildly adverse rooftop pressure gradient to improve wave drag and lift capabilities, but with a reduced extent of laminar flow. Careful consideration would be required to select/design an aerofoil section to achieve maximum aircraft efficiency and minimum operating economics with laminar flow and a suitable off-design performance. In addition, it is necessary to ensure adequate efficiency and economics with turbulent boundary layers.[8,10]

*3. Low-Speed Design*

In the case of a laminar aerofoil, because of its specific geometry (high curvature of the leading edge, rearward maximum cross section, etc.) and absence of leading-edge slats, special attention is required in high-lift conditions, mainly concerning prediction of leading-edge stall. The main feature of the flapped laminar airfoil is the dramatic loss in $\alpha_{\max}$ occurring when the flaps are deflected. This loss in $\alpha_{\max}$ is probably a consequence of the leading-edge type of stall, as expected from the small leading-edge radius. To increase $\alpha_{\max}$ capability, two alternatives can be considered[11,12]:

1) Compromise between low-speed and cruise can lead to greater value of leading-edge radius (can increase attachment line contamination possibility), compatible with acceptable value for $\alpha_{\max}$.

2) A leading-edge high-lift device (Krueger flap) can be used, but this will make the laminarization of the lower surface more difficult.

### C. Combined HLFC-VCW Configurations

*1. Cost Issues*

The main issue in the application of new technologies in transport aircraft is the ability to employ them at low cost without reduction of their benefits. This cost is reflected in the following elements of direct operating costs (DOC): fuel, ownership, and maintenance. Laminar-flow–variable-camber technology will only produce acceptable DOC if the penalties caused by additional weight and the complexity of the system do not exceed those of the fuel savings. Hence the most important objective in realizing advanced laminar-flow–variable-camber technology is to reduce their additional system costs and weight and minimize maintainability and reliability costs.

Laminar-flow flight research in the 1950s and 1960s demonstrated that manufacturing techniques needed to obtain the stringent surface smoothness and waviness criteria required for laminar-flow aircraft presented a major challenge. Today, it is recognized that conventional production aircraft wing surfaces can be built to meet these design constraints.[13]

*2. Combined HLFC-VCW Techniques for Flow Control on the Wing*

The most significant advance made in the development of the laminar-flow technology is the concept of hybrid laminar-flow control, an idea that integrates the concepts of NLF and LFC. It avoids the undesirable characteristics of both. NLF is sweep limited, and full-chord LFC is very complex. The key features of HLFC are 1) conventional spar box construction techniques are utilized, 2) boundary-layer suction is required only in the leading edge, 3) natural laminar flow is obtained over the wing box through appropriate tailoring of the geometry, and 4) the HLFC wing design has good performance in the turbulent mode. Typical aircraft drag reductions of around 10–11% are expected for this approach.[4,13] The leading-edge flight test on the NASA Jetstar aircraft addressed HLFC leading-edge system integration and reliability questions and set the stage for a commercial transport demonstration of HLFC.[14]

Practical use of HLFC requires that laminar flow is maintained through a range of cruise lift coefficients and Mach numbers. Variations in lift coefficient and Mach number will change the wing pressure distributions from the optimum and can result in some loss of laminar flow. It was therefore decided to investigate a HLFC wing together VC flap. Deflection of the VC flap permits controlling the pressure distribution over the forward part of the airfoil, keeping it similar to the design pressure distribution, even when the lift coefficient and Mach number differ considerably from the design values.[4] With careful design of a VC flap, it can be used to reduce the wave drag penalty and to sustain attached flow in the turbulent mode.[2] Flow control on such a wing is shown in Fig. 3.

*3. Candidate Combined HLFC-VCW Section Configurations*

Section views of the two wing configurations considered in this studies are shown in Fig. 4. Configuration I has both upper- and lower-surface suction, from the front spar forward with leading-edge systems as proposed by Lockheed.[14] It has no leading-edge devices, and so requires double-slotted Fowler flaps to achieve $C_{L_{\max}}$

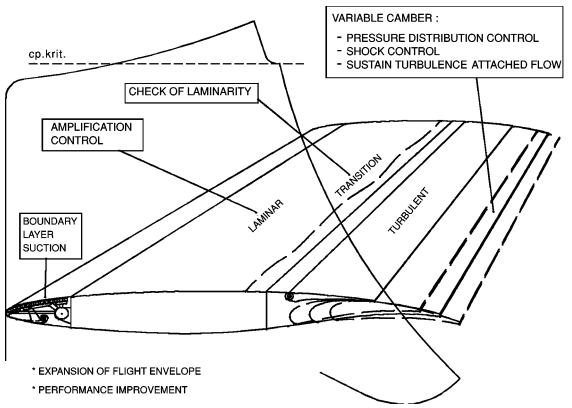


**Fig. 3 Flow control on the wing.**

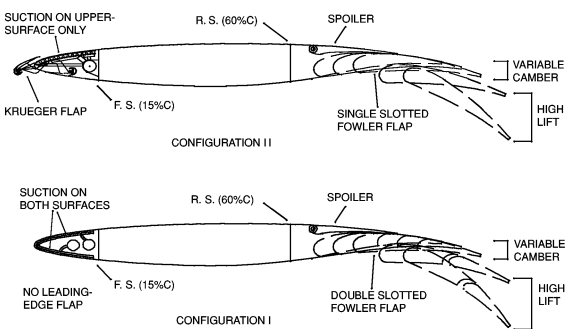


**Fig. 4 Cross sections of candidate combine HLFC-VCW configurations.**

requirements. Configuration II replaces the lower surface suction with full-span Krueger flaps, which, combined with single-slotted Fowler flaps, provide an equivalent high-lift capability. The Krueger flaps also shield the fixed leading edge from insect accumulation and provide space for the anti-icing system. The upper surface is the only one with suction panels. The leading-edge system used on configuration II is similar as proposed by Douglas.[15]

A summary of the advantages, risks, and disadvantages is as follows:

*Configuration I:* the advantages are that it is a simple system with no leading-edge devices, and it has upper- and lower-surface laminar flow for least drag. The disadvantages and risks are of more potential for insect contamination on the suction devices, which can cause boundary-layer transition. It leads to high approach speeds and landing field lengths and/or a more complex trailing-edge high lift system. It has longer takeoff field lengths, particularly for hot, high-altitude conditions, and has a trim penalty caused by higher rear loading (when the flaps are deployed).

*Configuration II:* the advantages are less potential insect contamination on the suction device; hence, the laminar boundary layer will be more stable. It has simpler trailing-edge high lift devices, lower approach speeds and shorter takeoff and landing field lengths, and smaller trim penalty when the flaps are deployed. The disadvantages are less drag reduction as a result of laminar flow being only on the upper surface and a more complex leading-edge system.

Preliminary estimates by Boeing[4] indicated cruise drag reductions of about 11% for HLFC having laminar flow on the upper and lower surfaces, whereas the reduction for HLFC having laminar flow only on the upper surface was only 7%. The deficiencies noted for configuration I are related to low-speed performance and insect contamination problems. The potential exists for high lift performance improvements if wings are specifically designed for the HLFC task. Although it has an inherently lower drag reduction, configuration II is more likely to provide a stable laminar boundary layer caused by a lower likelihood of being contaminated by insects. Taking into account the preceding considerations, configuration II was selected, for this study, but results for both configurations are shown later, for completeness.

#### 4. *Combined HLFC-VCW Section Baseline Configurations*

The HLFC-VC section baseline configuration used in this work is shown in Fig. 5. The leading-edge system used on this configuration is similar to leading-edge systems as proposed by Douglas,[15] while the variable-camber concept is described in the following paragraphs.

Ideally the change in section profile aft of the rear spar should not cause separation of airflow, which would otherwise give rise to higher profile drag. To overcome the problem of separation, the radii of local curvature must be greater than half the chord,[6] but not too high, as the section will have a higher pitching moment, and hence higher trim drag, which then will reduce the benefit of variable camber itself. The radii should be optimized between these two constraints. The radius is inherent in the trailing-edge upper surface of the aerofoil, so that when the aerofoil is used for a VC concept the aerofoil should be designed taking into account the preceding considerations from the beginning.

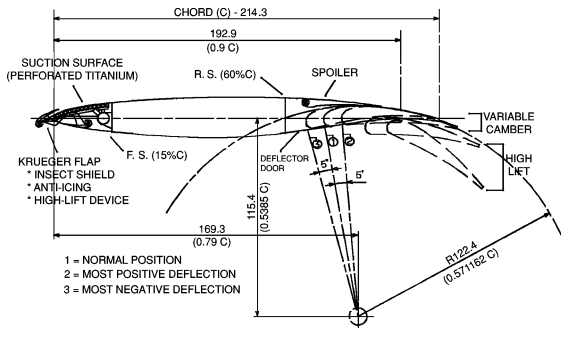


**Fig. 5 HLFC-VC section baseline configuration.**

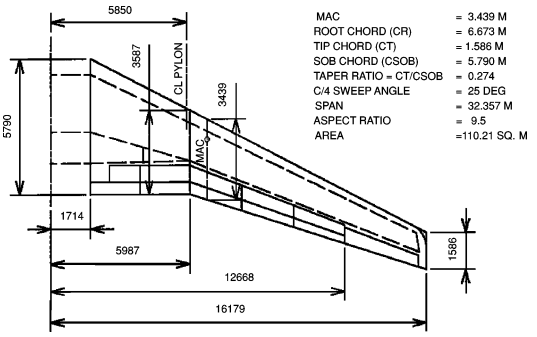


**Fig. 6 W-ATRA wing concept.**

The concept of variable camber used for this configuration is quite similar to traditional high-lift devices. To keep the systems simple, the camber variation is achieved by small rotation motions (in two directions for positive and negative deflections). In high-speed, low-deflection VC operation the flap body slides between the spoiler trailing edge and the deflector door. The radius of flap rotation is picked up from the radius of curvature of the aerofoil trailing-edge upper surface at about 90% chord. Camber variation is therefore performed with continuity in surface curvature at all camber settings. During this process, the spoiler position is unchanged. This concept also has been proposed by Greff,[2] but camber variation is achieved by Fowler motion, instead of rotation.

### D. Development of Three-Dimensional Geometry

For this study, a wing of a typical regional aircraft (W-ATRA) was sized[3] as shown in Fig. 6.

An inverse code suitable for use as a design tool was not available at Cranfield University during the course of the study. A generic analysis code, however, could be utilized (i.e., RAMPANT, for its verification see Sec. III.E.1), offering two- and three-dimensional, inviscid/viscous and incompressible/compressible capabilities).

Experience shows that it is best to begin with a subcritical design case.[4] To get good results from a subcritical design code such as SWEPTDES,[16] the target pressure distribution also must be subcritical. Despite the simplification afforded by use of a subcritical analysis, it was used to design the wing iteratively.

Subcritical pressure distributions corresponding to candidate aerofoils were then computed by SWEPTDES. These pressure distributions were then adjusted to meet the requirements already discussed (see Sec. III.B.2). A SWEPTDES aerofoil design computer program was then used to design a set of wing sections, plus a twist distribution that gave the required spanwise lift variation. A preliminary transonic analysis was then undertaken using RAMPANT.

#### 1. *Aerodynamic Design Objectives*

The main objectives of the wing design, which incorporates HLFC and VCW technology are the following:

a) The first is to obtain a pattern of approximately straight isobar sweep at an angle at least equal to the wing sweepback angle, with the upper surface generally being critical for drag divergence. If this aim is achieved, the flow will be approximately two dimensional, and the drag divergence will occur at the same Mach number everywhere along the span.

b) To obtain the greatest possible amount of laminar flow on the wing, this will significantly improve wing efficiency (lift-to-drag ratio) in cruise flight. The maximum reduction in drag for the wing must be obtained for the cruise $C_L$ corresponding to the design case for the proposed aircraft. To achieve the laminar-flow objectives for the design, it was required that the pressure distributions determined in Sec. III.B.2 (suitably interpolated over the span) should be realized by the three-dimensional wing.

c) The last is to have a good performance in off-design operations.

#### 2. *Outboard-Wing Design*

The design goals of the outboard aerofoil section used in the W-ATRA wing were 1) to sustain laminar flow to 55% chord (or more)

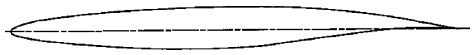

**Fig. 7 Profile of the outboard-wing aerofoil section.**

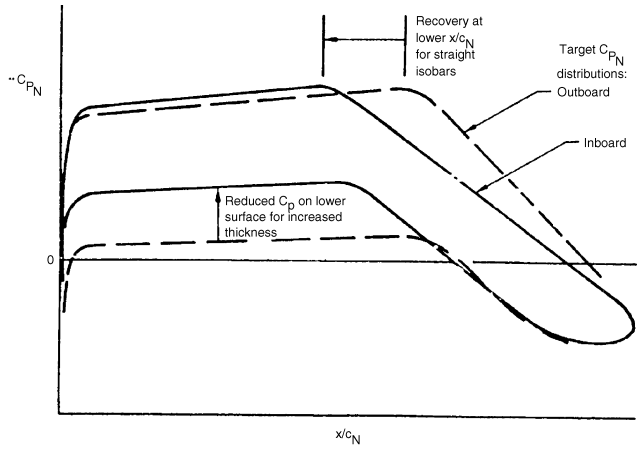


**Fig. 8 Root section pressure distribution considerations.**

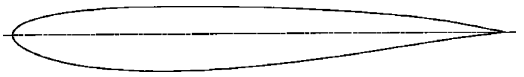

**Fig. 9 Profile of the root wing aerofoil section.**

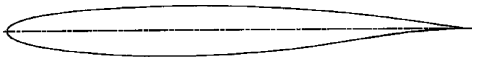

**Fig. 10 Profile of the inboard wing aerofoil section.**

on the upper surface with minimum suction and 2) to suffer little or no flow separation or wave drag at cruise Mach number of 0.8, wing lift coefficient 0.5, and 25 deg quarter-chord sweepback.

The outboard aerofoil section, used for the Boeing 757 HLFC research,[4] was used as starting point. This aerofoil was designed for a typical outboard section at a normal Mach number $M_N$ of 0.744, reflecting a sweepback angle of 21.5 deg, corresponding approximately to the 50% chord line outboard. The design lift coefficient ($C_{l_N}$, based on the normal flow) was 0.64, and the airfoil thickness-chord ratio ($t/c$) was 10.3%.

To facilitate the design process, the outboard-wing thickness distribution was chosen to be constant, and, therefore, a constant airfoil section is used in generating the outboard-wing geometry. Figure 7 shows the profile (streamwise) of the outboard-wing aerofoil section.

*3. Wing-Root Design*

The root section for the W-ATRA wing, a higher thickness ratio, was required. To keep the same maximum local Mach number on the upper surface, the pressure on the lower surface had to fall, thus reducing $C_{l_N}$. The increased chord inboard of the planform break was consistent with smooth and monotonic spanwise loading variation. Maintaining isobar sweepback required shifting the upper surface-pressure recovery point forward. Figure 8 illustrates these differences. The design $C_{l_N}$ was 0.4. Note that the resulting profile will not produce this pressure distribution when located close to the fuselage in a real flow. It is only one step in the design of the three-dimensional wing geometry in this section. Figure 9 shows the profile (streamwise) of the root wing aerofoil section.

*4. Wing Inboard Design*

The middle (inboard) aerofoil section illustrates a transition shape in the part of the wing (between side of fuselage and planform break/kink) where thickness chord ratio $t/c$ is decreasing. Figure 10 shows the profile (streamwise) of the inboard-wing aerofoil section.

*5. Off-Design Operation Consideration*

Practical use of HLFC requires that laminar flow be maintained through a range of cruise lift coefficients and Mach numbers. Changes in lift coefficient and Mach number will change the wing pressure distributions from the optimum and can result in some loss of laminar flow. Therefore, the W-ATRA wing incorporates a VC-flap. Deflection of the VC flap permits control of the pressure distribution over the forward part of the airfoil, keeping it similar to the design pressure distribution even when the lift coefficients and Mach numbers differ considerably from the design values. The desired pressure gradient control can be achieved not only during cruise, but also during a significant portion of climb and descent. The design concept of the variable camber wing for this work is described in Sec. III.C.

### E. Computational-Fluid-Dynamic Analysis

Many aircraft operate at transonic speed, where part of the flowfield is subsonic and part is supersonic. At these speeds shock waves form on the wings, which cause an increase in drag and variable changes in lift. Multiple shock waves can develop and interact in ways that are difficult to predict, but that have large influences on lift and drag.

With detailed knowledge of the flowfield and shock-wave locations, designers can shape the wing to delay the transonic drag rise and increase the lift-to-drag ratio. These result in higher transonic cruising speeds and reduced fuel consumption.

This flowfield knowledge can be obtained by predicting the chordwise pressure and spanwise distributions and modifying them by geometry changes. The flow around the wing can thus be controlled.

The main objective of this part of the design process was to analyze whether the wing used in this work (which is described in Sec. III) fulfills the design objectives or not.

The transonic flow over the W-ATRA wing of a typical regional aircraft wing-body configuration (WB-ATRA) was calculated. The computation was performed using RAMPANT, an unstructured, multigrid flow solver. This section shows the verification used to show that RAMPANT was a suitable. A three-dimensional model of the preceding configuration was created using CATIA, and a corresponding grid was created using preBFC and Tgrid.

*1. RAMPANT Verification*

A study was made to verify the use of RAMPANT as a primary design tool in the design of combined VCW-HLFC. The verification was made both on two-dimensional and three-dimensional configurations.[3]

*a) Two-dimensional problem.* A laminar-flow airfoil NLF-5, developed by Boeing,[17] was selected for this study. This airfoil has a thickness/chord ratio of 10.1%, a design section lift coefficient of 0.5, and is intended to cruise at $M = 0.78$.

The comparison of pressure distribution of the NLF-5 airfoil between NASA[17] and RAMPANT is shown in Fig. 11. The results

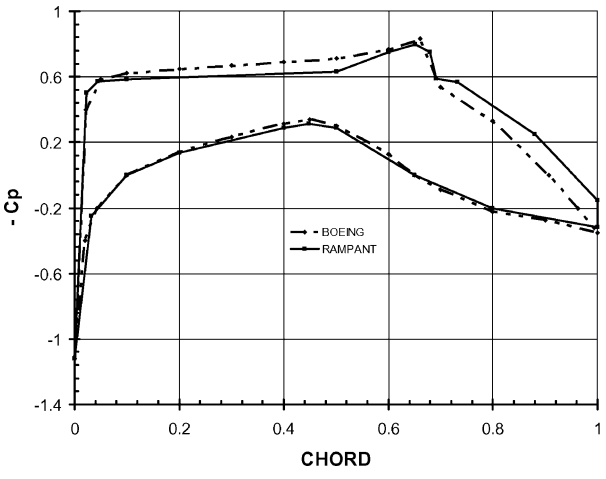


**Fig. 11 Pressure distribution of NLF-5 airfoil.**

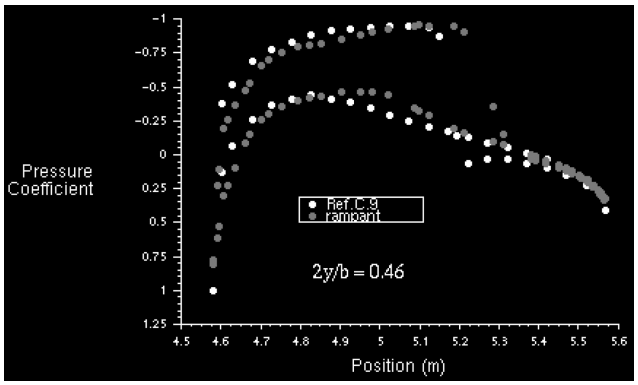


**Fig. 12 NACA 0012 wing pressure distributions (Ref. C.9 = Ref. 18).**

shown here are for $M_\infty = 0.78$, angle of attack = 0 deg, and Reynolds number of $20.6 \times 10^6$. The computational domain is a rectangular box that extends 25 chord lengths in front, behind, above, and below the airfoil. The NLF-5 airfoil mesh contains 6,218 nodes, 17,627 faces and 11,409 cells. Inviscid flow was assumed for the computations.

The pressure distribution predicted by RAMPANT is in fair agreement with the calculated data from NASA.[17] The shock position and strength are quite close. According to the RAMPANT predictions, the NLF-5 airfoil has more lift aft of the shock and less lift in the front of shock, hence more pitching moment.

*b) Three-dimensional problem.* The NACA 0012 wing, based on NASA,[18] was selected for this study. The wing has an aspect ratio of eight and a NACA 0012 airfoil, without twist. The planform has a taper ratio of 0.5 and a leading-edge sweep angle of 20 deg. The wing is attached to a cylindrical fuselage. (No fuselage geometry data are given.)

The comparison of pressure distributions at spanwise stations $(2y/b) = 0.46$ of the NACA 0012 wing between NASA[18] and RAMPANT is shown in Fig. 12. The results shown here are for $M_\infty = 0.85$, angle of attack = 2 deg, and Reynolds number based on the mean aerodynamic chord of $9 \times 10^6$. The computational domain is a rectangular box that extends 8.3 fuselage lengths in front, behind, above, and below the wing, and 7.8 wing semispans to the side of the wing. The domain mesh contains 55,593 nodes, 556,852 faces, and 267,874 cells. Inviscid flow was assumed for the computations.

The pressure distribution predicted by RAMPANT at spanwise station 0.46 is in fair agreement with the calculated data by TIBLT (transonic interactive boundary-layer theory[18]) code. A shock is present on the upper surface of the wing. The shock position predicted by RAMPANT is about 5% of the chord length aft of the TIBLT prediction. This might be because the grid is not fine enough (because the limitations of available computer memory) to capture the shock.

*c) Grid density comparison.* The following information on the grid density for similar studies can be used as comparisons with the preceding analysis. Simulations for NLR7301 airfoil were performed for the measurements obtained at the corrected experimental flow conditions of freestream Mach number of 0.753 and Reynolds number of $1.727 \times 10^6$ at an angle of attack of $-0.8$ deg (Ref. 19). The computational grids are C-type $257 \times 41$ and $257 \times 91$ points grids, respectively, for inviscid and viscous computations, respectively. The grids have minimum normal spacing at the airfoil surface of $1 \times 10^{-3}$ and $1 \times 10^{-6}$ chords, respectively, for inviscid and viscous computations, with 41 grid points in the wake and with far-field boundary extended by 25 chord lengths from the airfoil surface.

Numerical investigations for a wing with high-lift devices (slat and flap) were performed at Mach number of 0.22 and a chord-based Reynolds number of $3.7 \times 10^6$ at an angle of attack of 10 deg (Ref. 20). The simulation was using 10 chords upstream and 10 chords downstream. Structured, overset grids are used throughout this study. The flap zone used $185 \times 40 \times 75$ points, the slat zone used $121 \times 53 \times 27$ points. The flapped main element grid used $237 \times 40 \times 81$ nodes; the unflapped element grid used $187 \times 56 \times 115$ nodes. A slat box for tip vortex identification used a box of $63 \times 85 \times 100$ points. The composite mesh contains a total of 3.94 million points within eight zones. Mesh sizes for the two-element case and the full-span slat case are 2.31 million points and 3.02 million points, respectively.

### 2. *Configuration Description*

To simplify the problem and also to keep the grid size low as possible, the analysis was performed for a half-wing-body configuration only. Two flap configurations of HLFC-VC baseline configuration as shown in Fig. 5 were used in this analysis, that is, a) configuration I: VC flap undeployed [VC-flaps deflection or deflection of variable-camber wing (dvcw) along the span = 0 deg]; and b) configuration II: VC flap deployed (VC-flaps deflection or dvcw along the span are varied).

VC-flap deflection for configuration II is shown in Table 1. The variation of VC-flap deflection along the span is not optimized yet, but these analyses show the effect of VC-flap deflection on the section pressure distribution along the span.

The WB-ATRA's surface grid of configurations I and II used for this analysis was created. The grids are for $M_\infty = 0.8$, angle of attack = 0 deg, and Reynolds number of $21.6 \times 10^6$. The computational domain was a rectangular box that extends five fuselage lengths in front, behind, above, and below the wing, and three fuselage lengths (6.8 wing semispan) to the side of the wing. The size of the mesh of the preceding two configurations were as follows: a) configuration I = 35,019 nodes, 344,787 faces, 165,256 cells; and b) configuration II = 36,215 nodes, 355,903 faces, 170,522 cells.

Laminar flow was assumed for the preceding computations.

### 3. *Results*

The wing surface-pressure and Mach-number distributions were measured at six different spanwise stations: $2y/b = 0.106$, 0.191, 0.37, 0.578, 0.786, and 1.00. Figures 13 and 14 show pressure and Mach-number contours on the surface of configuration I. Figures 15

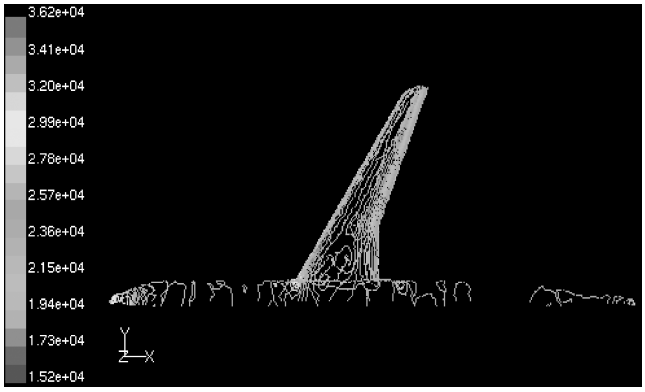


**Fig. 13 Configuration I: contours of static pressure, Pascal.**

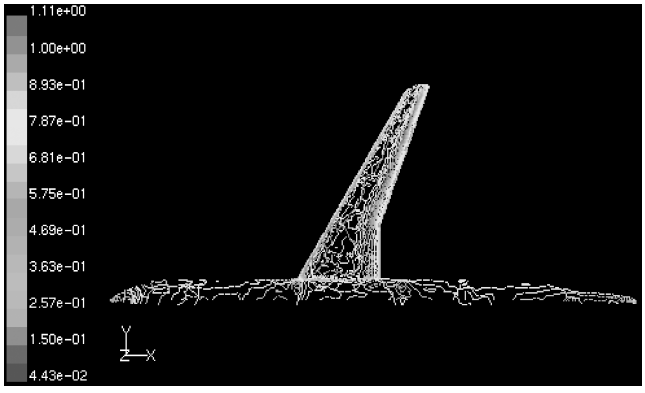


**Fig. 14 Configuration I: contours of Mach number.**

**Table 1 Section lift coefficients for configurations I and II**

| Wing section $x$ and $y$, m | SOB[a] | INB[b] | KINK[c] | SAOK[d] | SAOT[e] | STIP[f] |
|---|---|---|---|---|---|---|
| Spanwise station $y$, m | 1.714 | 3.236 | 5.986 | 9.350 | 12.713 | 16.719 |
| $2y/b$ ($b/2 = 16.179$ m) | 0.106 | 0.191 | 0.37 | 0.578 | 0.786 | 1 |
| Configuration I | | | | | | |
| Chord ($C$.I), m | 5.79 | 5.005 | 3.588 | 2.926 | 2.266 | 1.586 |
| Lift coefficient ($c_{l,I}$) | 0.258 | 0.298 | 0.38 | 0.439 | 0.343 | 0.24 |
| Configuration II | | | | | | |
| Chord ($C$.II), m | 5.873 | 5.082 | 3.649 | 2.96 | 2.239 | 1.558 |
| VC-flap deflection $d$, deg | 2 | 1.822 | 1.5 | 1 | −1 | −1.5 |
| Lift coefficient ($c_{l,II}$) | 0.387 | 0.395 | 0.4534 | 0.4935 | 0.3463 | 0.1889 |
| $C$.II/$C$.I | 1.0143 | 1.0153 | 1.017 | 1.0115 | 0.9882 | 0.9822 |
| $(c_{l,II}$-$c_{l,I})/d$, /deg | 0.0645 | 0.084 | 0.0489 | 0.0545 | −0.003 | 0.0341 |

[a]SOB = wing section at spanwise station 1.714 m.
[b]INB = wing section at spanwise station 3.236 m.
[c]KINK = wing section at spanwise station 5.986 m.
[d]SAOK = wing section at spanwise station 9.350 m.
[e]SAOT = wing section at spanwise station 12.713 m.
[f]STIP = wing section at spanwise station 16.719 m.

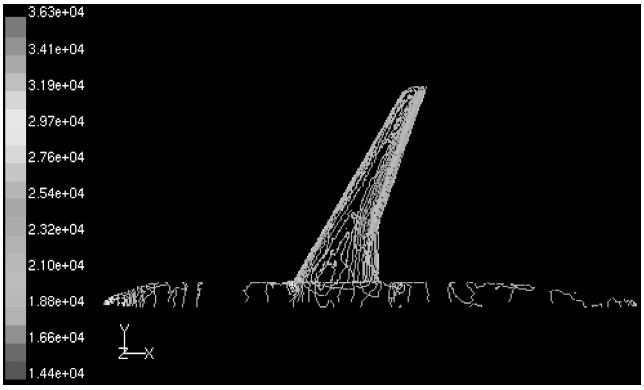


**Fig. 15 Configuration II: contours of static pressure, Pascal.**

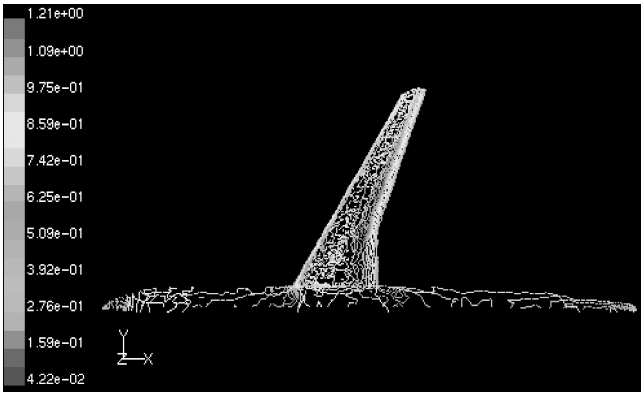


**Fig. 16 Configuration II: contours of Mach number.**

and 16 show pressure and Mach-number contours on the surface of configuration II.

The pressure and Mach-number distributions at spanwise stations: $2y/b = 0.106$, 0.191, 0.37, 0.578, 0.786, and 1.00 of configurations I and II are shown in Figs. 17 and 18.

From Figs. 13 and 15, for both configurations the average wing upper-surface isobar sweep angle (taken at 50% chord) is approximately 21.8 deg, instead of 25 deg (wing quarter-chord sweep angle). Thus, the isobar sweep efficiency is $= 21.8/25 = 0.872$. The inboard-wing upper-surface isobars are characterized by more sweeps forward at the front and less sweepback at the rear, and the shock strength is quite weak.

From Fig. 17, for configurations I and II, it can be seen that all of the pressure distributions (especially on the outboard wing, i.e., from the kink to the tip) are characterized by a steep initial gradient (rapidly falling pressure), followed by a negative pressure gradient (falling/favorable pressure) and a single weak shock wave and finally a recovery region with a soft aft pressure gradient. Based on guidelines of Sec. III.B.2, the preceding pressure distribution characteristics make it is possible to apply the HLFC concepts on the wing of configurations I and II.

As shown in Figs. 17 and 18, with the deflection of VC flap the pressure distribution shape at the front of shock does not change too much; this is good for HLFC application. The VC-flap deflection makes the shock stronger and increases aft loading (producing greater pitching moment and hence more trim drag).

The spanwise load distribution for configuration I (VC flap undeployed) and configuration II (VC flap deployed) are shown in Fig. 19.

At the aircraft design lift coefficient ($C_L = 0.5$), the comparisons between pressure distribution at subcritical Mach number and design Mach number for the outboard wing sections is shown in Fig. 20.

## IV. Discussion

The two-dimensional verification check showed that the pressure distribution predicted by RAMPANT was in fair agreement with the calculated data from NASA[17] (Fig. 11). The shock position and strength were quite close. The RAMPANT method predicted that the NLF-5 airfoil had more lift aft of the shock and less lift in the front of shock, hence more pitching moment.

The three-dimensional RAMPANT pressure distribution prediction at spanwise station 0.46 was in fair agreement with the calculated data by TIBLT[18] code (Fig. 12). A shock is present on the upper surface of the wing. The shock position predicted by RAMPANT was about 5% of the chord length aft of the TIBLT prediction. This might be because the grid was not fine enough (because the limitations of available computer memory) to capture the shock.

The W-ATRA wing configuration results were produced from only the first iteration of a very complex wing design process. The preceding wing is not yet optimum both for undeflected and deflected VC flap. Because of the limitations of time and computer memory, the first author cannot analyze the VC at several flight conditions (at design point as well as off design) to show its biggest benefit. Regardless of its weakness, its performance appears quite reasonable, and almost met the aerodynamic design objectives as described on Sec. III.D.1.

To improve the wing aerodynamic performance, it is recommended that further optimization be made of the airfoil sections, twist and VC-flap deflection distributions along the wing span, together with LFC suction requirements.

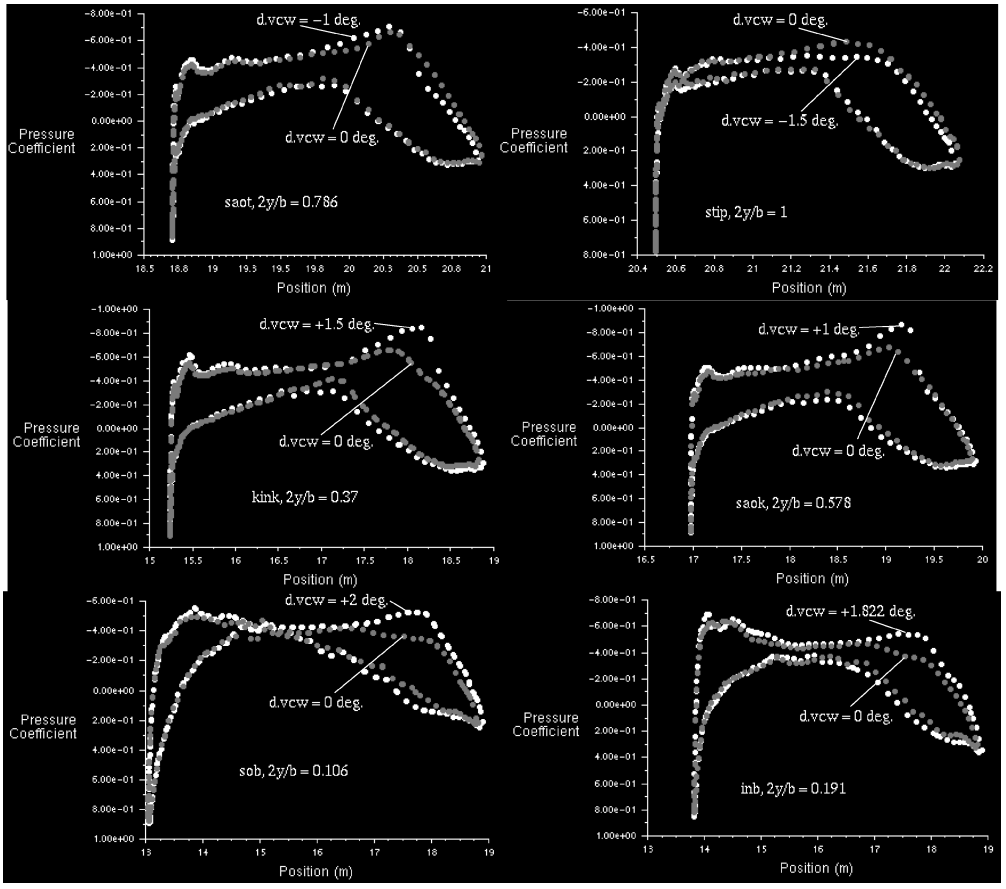


**Fig. 17 Configuration I (grey) and II (white): pressure distribution.**

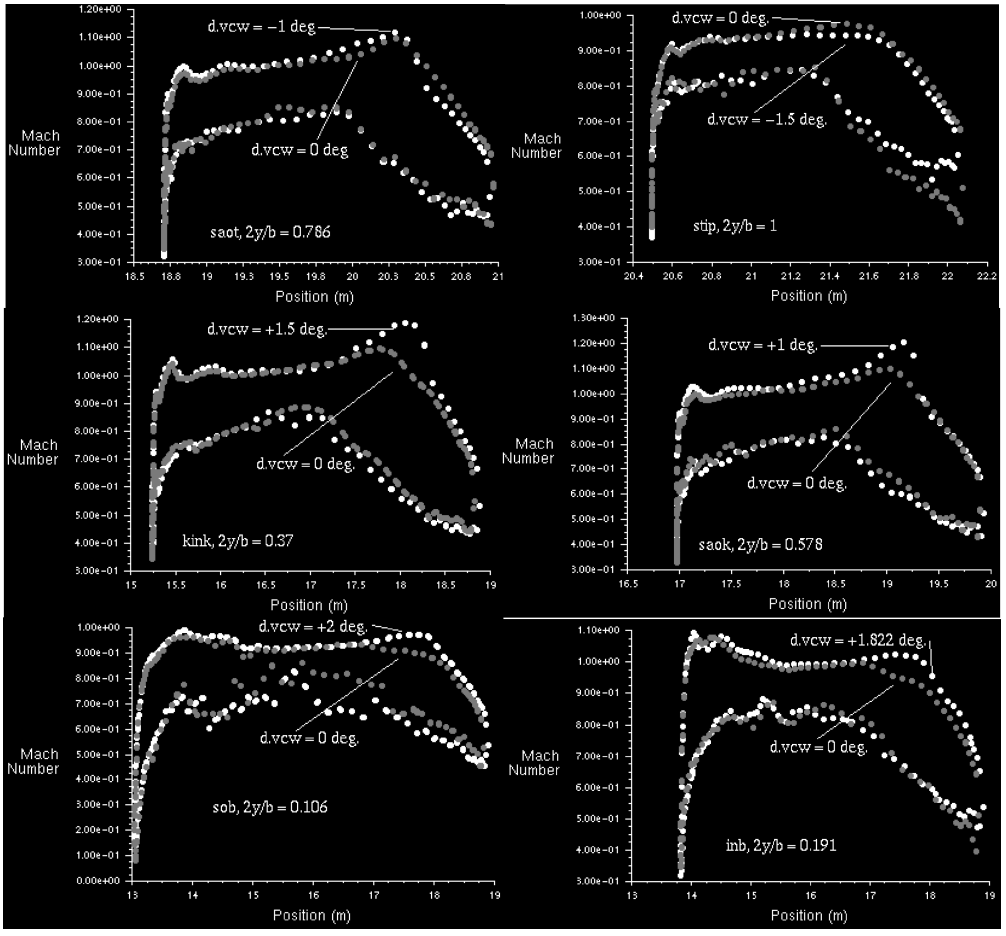


**Fig. 18 Configuration I (grey) and II (white): Mach-number distribution.**

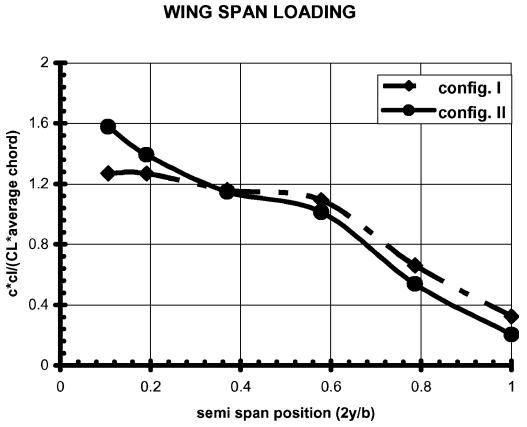


**Fig. 19 Wing span loading for configurations I and II.**

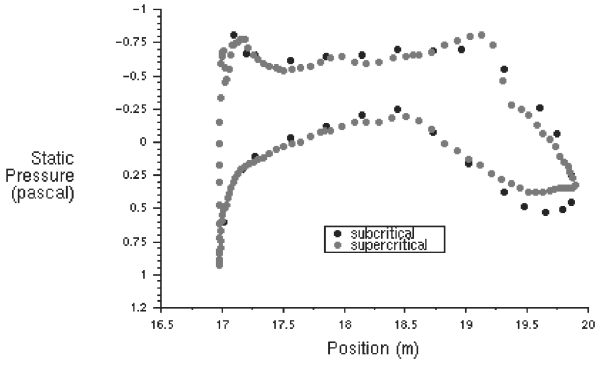


**Fig. 20 Comparisons between pressure distribution at subcritical Mach number and design Mach number for outboard-wing section (at $C_L = 0.5$).**

## V. Conclusions

A methodology has been developed for the aerodynamic wing design, allowing for the use of combined HLFC-VCW concepts for transonic transport aircraft.

The initial simple wing aerodynamic design process is reasonably accurate and is easy to perform (using SWEPTDES as a subcritical wing section design tool). This can be seen from the comparison with the RAMPANT (supercritical analysis) results.

To simulate the real flow, the grid should be fine enough, especially in the region of high curvature (e.g., leading edge), the grid adjacent to the wall, and in the regions of high pressure gradients.

The conclusion can finally be drawn that the combined HLFC–VCW concept is feasible for a transport aircraft from an aerodynamic point of view, with the same reservations that apply to the feasibility of any LFC aircraft, that is, that the economic aspects depend on manufacturing and operational data. Before HLFC and VCW technology can be applied to transport aircraft, a large multidisciplinary research effort is needed in order to master the technology and to demonstrate it on flying test beds and during in-service operational tests.

## Acknowledgments

The work presented in this paper was under funding from Indonesian Aerospace (IAe) and British Aerospace (BAe). We wish to thank B. J. Habbibie of IAe and Nick Beally of BAe for their support and encouragement.

## References

[1]Denning, R. M., Allen, J. E., and Armstrong, F. W., "Future Large Aircraft Design—the Delta with Suction," *The Aeronautical Journal*, Vol. 2212, May 1997, pp. 187–198.

[2]Greff, E., "Aerodynamic Design and Technology Concepts for a New Ultra-High Capacity Aircraft," International Council of the Aeronautical Sciences, Paper 96-4.6.3., Sept. 1996.

[3]Edi, P., "Investigation of the Application of Hybrid Laminar Flow Control and Variable Camber Wing Design for Regional Aircraft," Ph.D. Dissertation, AVT/CoA/Cranfield Univ., Cranfield, England, U.K., Sept. 1998.

[4]Boeing Commercial Airplane Co., "Hybrid Laminar Flow Control Study Final Technical Report," NASA CR 165930, Oct. 1982.

[5]Atkin, C. J., and Poll, D. I. A., "The Correlation Between Linear Stability Analysis and Cross Flow Transition near an Attachment Line," *Colloquium on Transitional Boundary Layers in Aeronautics*, Dec. 1995.

[6]Rao, A. J., "Variable Camber Wing for a Transport Aircraft," Ph.D. Dissertation, Dept. of Air Vehicle Design, CoA/Cranfield Univ., Cranfield, England, U.K., 1989.

[7]Redeker, G., and Wichmann, G., "Forward Sweep-a Favourable Concept for a Laminar Flow Wing," *Journal of Aircraft*, Vol. 28, No. 2, 1991, pp. 97–102.

[8]Wilson, R. A. L., and Jones, R. I., "Project Design Studies on Aircraft Employing Natural and Assisted Laminar Flow Technologies," Society of Automotive Engineers, Paper 952038, 1996.

[9]Wong, P. W. C., and Maina, M., "Study of Methods and Philosophies for Designing Laminar Flow Wings," ARA, Contractor Report M275/1, Bedford, England, U.K., Aug. 1995.

[10]Boeing Commercial Airplane Co., "Natural Laminar Flow Airfoil Analysis and Trade Studies Final Report," NASA CR 159029, Aug. 1977–June 1979.

[11]Capbern, P., "Theoretical and Experimental Study of High-Lift Device for a Natural Laminar Flow Airfoil," International Council of the Aeronautical Sciences, Paper 92-01-032, 1992.

[12]Morgan, H. L., "High-Lift Flaps for Natural Laminar Flow Airfoils," NASA CP-2413, 1985.

[13]Collier, F. S., Jr., "Recent Progress in the Development of Laminar Flow Aircraft," *ICAS Proceedings 1994, 19th Congress of the International Council of the Aeronautical Sciences*, Vol. III, Paper No. 94-4.7.1, Sept. 1994.

[14]Wagner, R. D., Maddalon, D. V., and Fisher, D. F., "Laminar Flow Control Leading-Edge Systems in Simulated Airline Service," *Journal of Aircraft*, Vol. 27, No. 3, 1990.

[15]Douglas Aircraft Co. Staff, "Evaluation of Laminar Flow Control System Concepts for Subsonic Commercial Transport Aircraft," NASA CR-159251, 1983.

[16]SWEPTDES, "A Computer Program of RAeS TDM 6312 for Calculating the Subcritical Inviscid Flow over a Finite Wing, with Compressibility Effects Updated to the Standard of ESDU TDM 7312."

[17]Boeing Commercial Airplane Co., "Natural Laminar Flow Airfoil Analysis and Trade Studies Final Report," NASA CR 159029, Aug. 1977–June 1979.

[18]Woodson, S. H., and DeJarnette, R., "A Transonic Interactive Boundary-Layer Theory for Laminar and Turbulent Flow Over Swept Wings," NASA CR 4185, 1988.

[19]Hussein, A. S., "Comparative Study Between Inviscid and Viscous Computations of Transonic Limit Cycle Oscillations for a Swept-back Supercritical Airfoil," *The International Journal of Intelligent Computing and Information Sciences (IJICIS)*, Vol. 4, No. 1, 2004, pp. 48–66.

[20]Baker, M. D., Mathias, D. L., Roth, K. R., and Cummings, R. M., "Numerical Investigation of Slat and Compressibility Effects for a High-Lift Wing," *Journal of Aircraft*, Vol. 39, No. 5, 2002, pp. 876–884.